

Concentrated oscillator strength of one-dimensional excitons in quantum wires observed with photoluminescence excitation spectroscopy

Hidefumi Akiyama, Takao Someya, and Hiroyuki Sakaki

Precursory Research for Embryonic Science and Technology (PRESTO) and Quantum Transition Project, Research Development Corporation of Japan and Research Center for Advanced Science and Technology, University of Tokyo, 4-6-1 Komaba, Meguro-ku, Tokyo 153, Japan

(Received 20 March 1996)

Photoluminescence excitation spectra have been measured on a series of T-shaped quantum-wire (T-QWR) samples fabricated by the cleaved-edge overgrowth method with molecular-beam epitaxy, in which the lateral confinement is systematically changed. We have successfully evaluated the absorption area intensity of one-dimensional (1D) excitons, and found the concentration of oscillator strength into 1D exciton states with increased lateral confinement. [S0163-1829(96)50924-0]

Oscillator strength of one-dimensional (1D) excitons in quantum wires (QWR's) has been one of the main subjects in the optical properties of semiconductor low-dimensional structures. Such study is particularly motivated by the expected concentration of oscillator strength into the lowest exciton state in QWR's as a result of the 1D electronic density of states concentrated at the low-energy edge¹ and the efficient Coulomb interaction among the carriers tightly confined.^{2,3}

The direct investigation of oscillator strength requires measurement of absorption and/or reflection intensity of QWR's, which, however, are difficult because of the small volume of the QWR structures. To attack this problem within photoluminescence (PL) and PL excitation (PLE) spectroscopy with higher sensitivity, careful study comparing a systematic series of QWR samples is required, since we can only partly know the relative intensities of the oscillator strength from these measurements. We report, in this paper, the structure dependence of PLE for three typical QWR samples, in which the lateral confinement is systematically changed. We have found the concentration of oscillator strength into 1D exciton states with increased lateral confinement.

For such systematic investigation, the T-shaped QWR (T-QWR) structure fabricated by the cleaved-edge overgrowth (CEO) method with molecular-beam epitaxy⁴ (MBE) has the following advantages. Since the T-QWR's are defined by the two kinds of quantum wells (QW's) formed separately with well-established MBE layer-growth technique, T-QWR's with arbitrary combination of QW's are possible to fabricate.⁴⁻⁶ Furthermore, the precise characterization technique of structures, energy levels, and wave functions has been established for T-QWR's.^{6,7} As for PLE of T-QWR's, we have so far studied one sample in detail,⁷ which is a 5-nm-scale GaAs T-QWR structure with AlAs barriers realizing tight lateral confinement. We clarified the confinement-induced optical anisotropy in T-QWR's. With a systematic series of samples, we now go to the interesting problem of the oscillator strength of 1D excitons.

The three T-QWR samples (A-C) studied here were fabricated by the CEO method with MBE. The inset of Fig. 1 shows the schematic structure of our T-QWR samples. The T-QWR's are formed at the intersection of multiple QW's

(denoted as QW1) grown in the first MBE growth on a GaAs (001) substrate and a QW (denoted as QW2) overgrown on the second MBE growth on a (110) surface prepared by *in situ* cleavage. All the QW layers are of GaAs, while the barrier layers are of Al_{0.3}Ga_{0.7}As, which is denoted in short form as the GaAs/Al_{0.3}Ga_{0.7}As structure. In making this series of samples, we performed the first growth simultaneously on one wafer and cut it into small pieces, on which three runs of CEO were done changing the overgrown-QW thickness. Therefore, the three samples have identical multiple-QW structure, which consists of 200 periods of QW1 with thickness $a=5.2$ nm and barriers with thickness $c=31$ nm. On the other hand, the thickness b of the overgrown QW's (QW2) is changed as $b=4.8$ nm in sample A, $b=6.9$ nm in sample B, and $b=10$ nm in sample C. More detailed description of sample preparation is given elsewhere.⁶

For these samples, we performed polarization-dependent

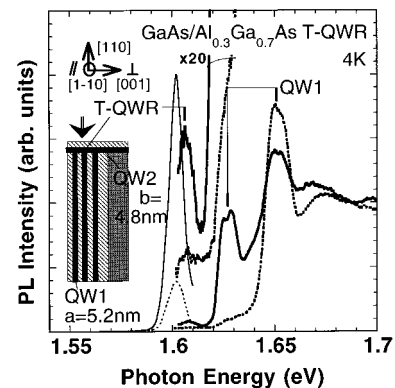


FIG. 1. PL (thin curves) and PLE (thick curves) spectra measured at 4 K for sample A (GaAs/Al_{0.3}Ga_{0.7}As T-QWR's, $a=5.2$ nm, $b=4.8$ nm). The polarization of the light for detection in PL and excitation in PLE was parallel (\parallel , solid curves) or perpendicular (\perp , broken curves) to the T-QWR's. The magnified PLE spectra by a factor of 20 are shown for the low-energy region. The inset shows the schematic structure of the T-QWR sample. Multiple QW's (QW1) are firstly grown on a GaAs(001) substrate and then cleaved *in situ* to prepare a fresh (110) surface, on which QW2 is secondly grown. The T-QWR states are formed at the T-junction parts of QW1 and QW2.

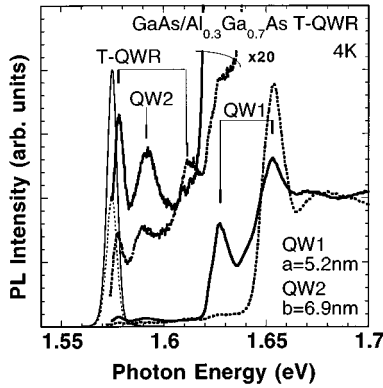


FIG. 2. PL (thin curves) and PLE (thick curves) spectra measured at 4 K for sample *B* (GaAs/Al_{0.3}Ga_{0.7}As T-QWR's, $a=5.2$ nm, $b=6.9$ nm) for polarizations parallel (\parallel , solid curves) and perpendicular (\perp , broken curves) to the T-QWR's.

PL and PLE measurements at 4 K with a cw titanium sapphire laser and a conventional micro-PL setup which is described in detail in a separate paper.⁷ The photoexcitation and the detection were made along the $[1\bar{1}0]$ direction via the (110) surface in the backward-scattering geometry under the normal-incidence condition. Note that the polarization of detected light was analyzed in the PL measurements, while that of excitation light was selected in the PLE measurements. We denote polarization along $[1\bar{1}0]$ ($[001]$) as \parallel (\perp), since $[1\bar{1}0]$ ($[001]$) is parallel (perpendicular) to the T-QWR's and the QW1 layers.

Figures 1–3 show PL and PLE spectra of samples A–C with the different QW2 thickness b . In each figure, a pair of peaks shown by thin curves in the low-energy region show the PL spectra of the 1D excitons confined in T-QWR's, and a pair of thick curves in the higher-energy region show their PLE spectra. The low-energy part of the PLE spectra magnified by a factor of 20 are also shown. In each pair of spectra, the solid curve is obtained for the polarization parallel to the T-QWR's, whereas the broken curve is for the polarization perpendicular to the T-QWR's. In the measurements for both polarizations, the detection sensitivity and the

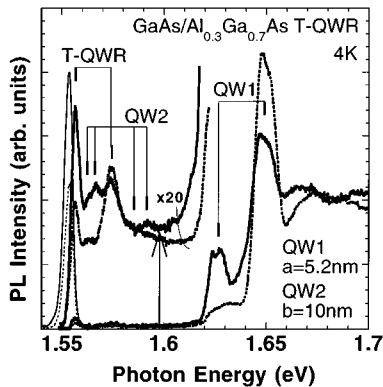


FIG. 3. PL (thin curves) and PLE (thick curves) spectra measured at 4 K for sample *C* (GaAs/Al_{0.3}Ga_{0.7}As T-QWR's, $a=5.2$ nm, $b=10$ nm) for polarizations parallel (\parallel , solid curves) and perpendicular (\perp , broken curves) to the T-QWR's. The PLE intensity for the continuum state of QW2 indicated by an arrow gives a measure of the absorption probability of 1.3%.

excitation intensity were kept constant. Furthermore, we set the scale of PLE spectra common among Figs. 1–3, as will be proven later. Thus, we can compare all the PLE intensities among Figs. 1–3.

Figure 1 shows the PL and PLE spectra of sample *A* (GaAs/Al_{0.3}Ga_{0.7}As T-QWR's, $a=5.2$ nm, $b=4.8$ nm). As indicated in the figure, the PL peaks at 1.602 eV and the lowest-energy PLE peaks at 1.606 eV are from the lowest exciton state at T-QWR's, while the larger PLE peaks at 1.627 eV and 1.651 eV are the heavy-hole (HH) and light-hole (LH) exciton states in QW1, respectively.⁸ Such large contributions of QW1 to the PLE spectra of T-QWR's are caused by a plentiful carrier flow from QW1 to T-QWR's. Structures associated with QW2 were not observed since they are located in the energy region higher than that of QW1 and are overshadowed by the much larger contributions of QW1. The strong polarization anisotropy observed in QW1 agrees well with the well-known optical anisotropy of HH and LH excitons in standard (001) QW's observed from the (110) cleaved surface,⁹ and that in T-QWR's agrees also well with our previous study on the GaAs/AlAs T-QWR sample ($a=5.3$ nm, $b=4.8$ nm).

Note here that these general features in Fig. 1 are similar to those of the GaAs/AlAs T-QWR sample previously reported in detail. This is because of the similarity in the parameters a and b , though the confinement is weaker due to the lower barriers in the present sample *A*. Due to the better heterointerface quality in the present GaAs/Al_{0.3}Ga_{0.7}As T-QWR's, however, their PL and PLE spectra are sharper, and the Stokes shift is smaller, than the GaAs/AlAs T-QWR sample of similar size. The PL linewidth (full width of half maximum) was 8.5 meV and the Stokes shift was 4 meV, representing the high quality of the sample. The effective lateral confinement energy of excitons E_{1D-2D}^* , which is defined as the energy difference between the 1D exciton in T-QWR's and the lowest 2D exciton in either QW1 and QW2, is found to be 21 meV in PLE spectra.

Figure 2 shows the PL and PLE spectra of sample *B* (GaAs/Al_{0.3}Ga_{0.7}As T-QWR's, $a=5.2$ nm, $b=6.9$ nm). Similarly to Fig. 1, the PL peaks at 1.575 eV and the lowest-energy PLE peaks at 1.578 eV are from the HH exciton state in T-QWR's, and the structure above 1.620 eV with two PLE peaks are from the HH and LH exciton states in QW1.⁸ The values of the PL linewidth and the Stokes shift of T-QWR's are smaller, 6.2 meV and 3 meV, respectively. Since the QW2 thickness b is increased in sample *B*, the PLE peaks of HH excitons in QW2 and the LH excitons in T-QWR's are also observed, as indicated in the figure. Thus, the effective lateral confinement energy of excitons E_{1D-2D}^* is now given by the energy distance between PLE peaks of QW2 and T-QWR's, and is found to be decreased to 14 meV, which shows that the T-QWR states take on 2D character.

The PL and PLE of HH excitons in T-QWR's is stronger for the parallel polarization, in agreement with our previous study. The PLE of LH excitons in T-QWR's shows opposite polarization dependence. These tendencies in optical anisotropy in T-QWR's are as expected and close to that in QW1, since the directions of confinement and free motion are common between T-QWR's and QW1.

We should note that the PLE intensity of HH excitons in T-QWR's is comparable with that of QW2,¹⁰ where their

area-intensity ratio is about 1:2. This ratio is to be compared with the following geometrical factors. The period of QWR's is given by $a+c=36$ nm, in which the wave functions of 1D excitons in T-QWR's are bounded at the T-junction parts to have some reduced lateral size. On the other hand, the 2D excitons denoted as QW2 are not bounded, but are extended over the period of 36 nm. Since the lateral size of 1D excitons is less than 18 nm, the PLE area-intensity ratio of 1/2 is larger than the geometrical size ratio for the 1D and 2D excitons. Also note that the period of 36 nm is much smaller than the carrier diffusion length in QW's ($\sim\mu\text{m}$), so that all the carriers generated at QW2 are quickly captured into T-QWR's. In such a case, the PLE intensity is proportional to the absorption intensity, and their energy-integrated area intensities are proportional to the oscillator strength. Therefore, the enhanced and reduced PLE area intensities of T-QWR's and QW2 compared with the geometrical factors suggest that the oscillator strength of excitons in QW2 is transferred to those in T-QWR's.

Figure 3 shows the PL and PLE spectra of sample C (GaAs/Al_{0.3}Ga_{0.7}As T-QWR's, $a=5.2$ nm, $b=10$ nm). Since the QW2 thickness b is further increased, the PLE peaks of HH and LH excitons in T-QWR's, QW2, and QW1 are all observed, as indicated in the figure. Both the PL linewidth and the Stokes shift of this T-QWR are smaller, 5.1 meV and 3 meV, respectively. As for the structures marked as QW2, they are attributed to the excitons delocalized over QW2; the lower two peaks at 1.563 eV and 1.566 eV to HH excitons, while the upper unclear structures marked at 1.585 eV and 1.592 eV to LH excitons. Details of their origin and their polarization dependence are not known. The effective lateral confinement energy of excitons $E_{1\text{D}-2\text{D}}^*$ is further decreased to 6 meV in PLE spectra, which shows that the T-QWR states are getting closer to QW2 states both in their energy and wave function.

It is interesting to point out that the PLE structure below 1.620 eV is from the step-function-like 2D density of states of QW2 except for the excitonic peaks at the low-energy edges, where the weakened excitonic peaks of QW2 and the strong excitonic peaks of T-QWR's are observed. This again demonstrates that the oscillator strength of excitons in QW2 is transferred to those in T-QWR's. As for the continuum state showing the 2D density of states of QW2, the absorption probability is known to be 1.3%,¹¹ which is indicated by an arrow in the figure. As already mentioned above, all the carriers absorbed by T-QWR and QW2 states are supposed to flow into the lowest exciton state in T-QWR's by the same efficiency, the PLE intensities of T-QWR and QW2 are proportional to the absorption probability. Therefore, the absorption probability of 1.3% for the continuum state of QW2 is a useful standard in evaluating the absorption probability at T-QWR's, which we discuss below.

The central issue of this paper is the comparison of the PLE peak intensities among Figs. 1–3, especially for HH excitons in T-QWR's. It is true that PLE signal intensities depend on all the absorption, energy relaxation, and/or carrier migration processes, and the detection condition of PL, which can be different in the three figures. Note, however, that the first growth parts with QW1 in samples A–C are cut from the same wafer and have identical properties, and hence that the carrier supply from QW1 to T-QWR's is identical

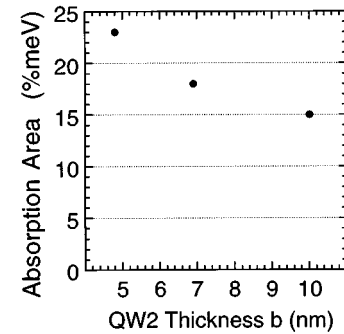


FIG. 4. The enhancement of absorption area intensity of HH excitons in T-QWR's with reduced QW2 thickness b , observed in samples A, B, and C (QW1 thickness $a=5.2$ nm, QWR period $a+c=36$ nm). Since lateral confinement is stronger for smaller b , the lateral size of the exciton wave function, and hence the cross-sectional area for the incident light, are smaller for smaller b . Thus, the local oscillator strength obtained by normalizing each datum by the lateral size is to be significantly enhanced for smaller b .

for the three samples. Thus, we can compare the relative PLE intensities of the overgrown parts in the three samples, by setting the scale of PLE spectra in Figs. 1–3 such that the PLE structures of QW1 have common amplitude. Furthermore, the PLE intensity for the continuum state of QW2 indicated by an arrow in Fig. 3 gives the standard of the absorption probability of 1.3%.¹¹ Therefore, we can evaluate absolute absorption probabilities at T-QWR's from the PLE intensities in Figs. 1–3.

The peak absorption probabilities of HH excitons in T-QWR's in the three figures are then evaluated to be 2.7%, 2.9%, and 3.0%, for samples A, B, and C, respectively, all with the T-QWR period of 36 nm. Multiplying the linewidth, we obtain the absorption area intensities of three samples, which are 23% meV, 18% meV, and 15% meV, respectively, and are plotted in Fig. 4. This shows that the oscillator strength is largest in sample A, which is with the strongest lateral confinement among the three samples. Note that the lateral size of the exciton wave function is smallest in sample A, or that the cross-sectional area for the incident light is smallest, which should contribute to *reduce* the PLE intensity. That is to say, if we normalize the obtained relative oscillator strength by the cross-sectional area for the incident light, we obtain significant enhancement of the local oscillator strength in sample A. We can conclude that the oscillator strength is not only enhanced, but also highly concentrated spatially at the T-junction part, when the lateral confinement is strong.

The lateral sizes of exciton wave functions in T-QWR's and QW2 in respective samples are not yet quantitatively evaluated. Thus, we are not able to normalize the observed oscillator strength with the sizes to quantify the local oscillator strength concentrated to the T-QWR's and to compare it with that of QW2. In addition, no theoretical model is currently available to quantitatively explain the increased oscillator strength with lateral confinement and the oscillator strength transfer from QW2 to T-QWR's. Hence, the quantitative analyses as well as the physical interpretation on the concentration of oscillator strength are the subject of future study.

We comment here on the recent PLE work on 10-nm-scale or even smaller QWR's with strong lateral confinement. Previously, PLE measurements of such small QWR's have been difficult, because their PLE peaks tend to broaden and overlap with other spectral structures. Only recently, clear PLE spectra of such QWR's have appeared thanks to the improvements in the quality of QWR samples^{7,12} or in characterization technique.¹⁰ For the quantitative analysis of the oscillator strength of QWR's with PLE, however, systematic study on a series of high-quality samples is required. We believe that the present work on T-QWR's is the first demonstration to evaluate the absorption probability of 1D excitons in semiconductor QWR's.

In conclusion, three typical T-QWR samples were fabricated by the CEO method, in which the lateral confinement is systematically changed. We have studied these samples with PLE spectroscopy, and found that the oscillator strength of the 1D exciton states is enhanced and spatially concentrated with increased lateral confinement. The absorption area intensity was 23% meV for the lowest HH excitons in GaAs/Al_{0.3}Ga_{0.7}As T-QWR's formed by the 5.2-nm- and 4.8-nm-thick QW's with a period of 36 nm.

This work was partly supported by a Grant-in-Aid from the Ministry of Education, Science, Sports, and Culture, Japan.

¹Y. Arakawa and H. Sakaki, Appl. Phys. Lett. **40**, 939 (1982).

²R. Loudon, Am. J. Phys. **27**, 649 (1959); R. J. Elliott and R. Loudon, J. Phys. Chem. Solids, **15**, 196 (1960).

³T. Ogawa and T. Takagahara, Phys. Rev. B **44**, 8138 (1991).

⁴L. N. Pfeiffer, K. West, H. L. Störmer, J. P. Eisenstein, K. W. Baldwin, D. Gershoni, and J. Spector, Appl. Phys. Lett. **56**, 1697 (1990).

⁵W. Wegscheider, L. N. Pfeiffer, M. M. Dignam, A. Pinczuk, K. W. West, S. L. McCall, and R. Hull, Phys. Rev. Lett. **71**, 4071 (1993).

⁶T. Someya, H. Akiyama, and H. Sakaki, J. Appl. Phys. **79**, 2522 (1996); Appl. Phys. Lett. **66**, 3672 (1995); Phys. Rev. Lett. **74**, 3664 (1995); **76**, 2965 (1996).

⁷H. Akiyama, T. Someya, and H. Sakaki, Phys. Rev. B **53**, 4229 (1996).

⁸The $j=3/2$ hole states in bulk GaAs are separated into heavy-hole (HH) and light-hole (LH) states in QWR's and QW's, resulting in the HH and LH excitons. Consistently with the usual notation, we use the term heavy or light in the sense that it has heavier or

lighter effective mass in the confinement direction in QW's and QWR's to give smaller or larger quantization energy for holes. Thus, the lowest-energy excitons and higher-energy excitons in QWR's and QW's are classified as HH and LH excitons, respectively.

⁹J. S. Weiner, D. S. Chemla, D. A. B. Miller, H. A. Haus, A. C. Gossard, W. Wiegmann, and C. A. Burrus, Appl. Phys. Lett. **47**, 664 (1985).

¹⁰A similar effect has been recently demonstrated with near-field scanning optical microscopy in a strained QWR system; T. D. Harris, D. Gershoni, R. D. Grober, L. Pfeiffer, K. West, and N. Chand, Appl. Phys. Lett. **68**, 988 (1996).

¹¹Y. Masumoto, M. Matsuura, S. Tarucha, and H. Okamoto, Phys. Rev. B **32**, 4275 (1985).

¹²E. Kapon, G. Biasiol, D. M. Hwang, M. Walther, and E. Colas, in *Proceedings of the 7th International Conference on Modulated Semiconductor Structures, Madrid, Spain, 1995*, edited by L. Viña *et al.* [Solid State Electron. (to be published)].